

# Estimating evapotranspiration using the complementary relationship and the Budyko framework

Homin Kim and Jagath J. Kaluarachchi

## ABSTRACT

Several models have been developed to estimate evapotranspiration. Among those, the complementary relationship has been the subject of many recent studies because it relies on meteorological data only. Recently, the modified Granger and Gray (GG) model showed its applicability across 34 diverse global sites. While the modified GG model showed better performances compared to the recently published studies, it can be improved for dry conditions and the relative evaporation parameter in the original GG model needs to be further investigated. This parameter was empirically derived from limited data from wet environments in Canada – a possible reason for decreasing performance with dry conditions. This study proposed a refined GG model to overcome the limitation using the Budyko framework and vegetation cover to describe relative evaporation. This study used 75 eddy covariance sites in the USA from AmeriFlux, representing 36 dry and 39 wet sites. The proposed model produced better results with decreasing monthly mean root mean square error of about 30% for dry sites and 15% for wet sites compared to the modified GG model. The proposed model in this study maintains the characteristics of the Budyko framework and the complementary relationship and produced improved evapotranspiration estimates under dry conditions.

**Key words** | Budyko framework, complementary relationship, evapotranspiration, NDVI

**Homin Kim** (corresponding author)  
Utah Water Research Laboratory,  
Utah State University,  
1600 Canyon Road,  
Logan,  
UT 84321,  
USA  
E-mail: [homin.kim@aggiemail.usu.edu](mailto:homin.kim@aggiemail.usu.edu)

**Jagath J. Kaluarachchi**  
College of Engineering,  
Utah State University,  
4100 Old Main Hill,  
Logan,  
UT 84322-4100,  
USA

## INTRODUCTION

Estimating evapotranspiration ( $E_T$ ) is an essential part of agricultural water management and there are many classical methods available for  $E_T$  estimation based on data availability and required accuracy. The original models include the Penman (1948) and Penman–Monteith (Monteith 1965) equations that combine energy balance and aerodynamic water vapor mass transfer principles. In recent years, the Food and Agriculture Organization (FAO) version of the Penman–Monteith equation (Allen *et al.* 1998) has been widely used to estimate  $E_T$ . According to Morton (1994), the Penman–Monteith equation is limited for hydrologic purposes. For example, meteorological data are not measured at 2 m elevation from ground level and not at crop elevation, as required by the Penman–Monteith

equation (Shuttleworth 2006). Also, the FAO method is primarily used to estimate crop  $E_T$  from agricultural lands using crop coefficients which are estimated under specific environmental conditions and at specific times of the growing cycle. According to Shuttleworth & Wallace (2009), this extrapolation is questionable while information of crop coefficients and growing cycles are not readily available worldwide.

Another approach to estimate  $E_T$  directly is the complementary relationship developed by Bouchet (1963). This approach proposed the first complementary function of potential evapotranspiration ( $E_P$ ) and wet environment evapotranspiration ( $E_W$ ) for a wide range of available energy to estimate regional  $E_T$ . Bouchet (1963) postulated that as a wet

surface dries, the decrease in evapotranspiration is matched by an equivalent increase in potential evapotranspiration.  $E_p$  is evaporation from a saturated surface while energy and atmospheric conditions do not change.  $E_w$  is the value of potential evaporation when actual evaporation is equal to the potential rate. Bouchet's idea has been widely tested in conjunction with the models of Priestley & Taylor (1972) and Penman (1948). Examples of widely known models using the complementary relationship are the advection-aridity (AA) model of Brutsaert & Stricker (1979), the complementary relationship areal evapotranspiration (CRAE) model of Morton (1983), and the complementary relationship model proposed by Granger & Gray (1989) which is named as the GG model hereafter. In these three models,  $E_T$  is usually calculated by Equation (1), developed by Bouchet (1963):

$$E_T + E_p = 2E_w \quad (1)$$

The procedure to calculate  $E_T$ , which requires only meteorological data, was proposed by Brutsaert & Stricker (1979).

In the AA model,  $E_p$  is estimated by combining information from the energy budget and water vapor transfer in the Penman (1948) equation. The partial equilibrium evapotranspiration equation of Priestley & Taylor (1972) was used to calculate  $E_w$ . In the CRAE model of Morton (1983), the Penman equation is divided into two separate terms representing the energy balance and the vapor transfer process to calculate  $E_p$ . A refinement to this approach is proposed through the definition of 'equilibrium temperature',  $T_p$ , which is the temperature at which the energy budget method and the mass transfer method for a moist surface yields the same  $E_p$ . In the calculation of  $E_w$ , Morton (1983) modified the Priestley & Taylor equilibrium evapotranspiration to explain the temperature dependence of both net radiation and the slope of the saturated vapor pressure curve. In the GG model of Granger & Gray (1989), they proposed a revised version of the Penman's equation for estimating  $E_T$  from different saturated and non-saturated surfaces using a dimensionless relative evaporation parameter for a given set of atmospheric and surface conditions. Later, they showed that relative evaporation, the ratio of actual to potential evapotranspiration,

has a unique relationship with a parameter which they called relative drying power using 158 measurement data points from Canada. This relationship is independent of surface parameters (temperature and vapor pressure). The primary advantage of the GG model is that  $E_T$  can be directly estimated without the surface parameters or prior estimates of  $E_p$ . The original GG model has been successfully applied to a wide range of physical and surface conditions (Hobbins *et al.* 2001; Szilagyi & Jozsa 2008).

Although Equation (1) of Bouchet (1963) has been widely used in conjunction with Penman (1948) and Priestley & Taylor (1972) (Brutsaert & Stricker 1979; Morton 1983; Hobbins *et al.* 2001), Bouchet (1963) assumed that  $E_p$  decreases by the same amount as  $E_T$  increases. Granger (1989) argued that the symmetrical relationship of Equation (1) lacked a theoretical background and showed the symmetrical relationship only occurs near a temperature of 6 °C. This earlier study showed that  $E_T$  and  $E_p$  contribute to  $E_w$  with different coefficients that depend on the psychrometric constant and the slope of the saturation vapor pressure curve. Later, Crago & Crowley (2005) evaluated the Granger (1989) equation by comparing it to measured latent heat fluxes and determined that the radiometric surface temperature measurements can be successfully incorporated into a complementary approach of Granger (1989). Kahler & Brutsaert (2006) incorporated a constant parameter,  $b$ , into the energy balance equation. The parameter  $b$  is dependent on the response of natural evaporation from the surrounding landscape. They showed that  $b$  values around 5 may be appropriate for the complementary relationship. Venturini *et al.* (2008, 2011) evaluated the approach of Granger & Gray (1989) along with the Priestly and Taylor equation. In their studies, the relative evaporation parameter in the GG model was derived from surface temperature of MODIS data and produced errors of about 15% compared to observed  $E_T$ . In essence, these studies support the complementary relationship, but confirmed that it requires improvements to better predict  $E_T$ .

Recently, Anayah & Kaluarachchi (2014) developed a modified method using the complementary method proposed by the GG model with meteorological data from 34 global eddy covariance (EC) sites. These sites were distributed as follows: North America (17), Europe (11), Asia (5),

and Africa (1). The results of this modified GG model showed that the average root mean square error decreased from 20% to as much as 80% compared to the recently published work of Suleiman & Crago (2004), Mu *et al.* (2007, 2011), Szilagyi & Kovacs (2010), Han *et al.* (2011), and Thompson *et al.* (2011). While the results of Anayah & Kaluarachchi (2014) were very good, the results also showed that further refinements can improve performance under dry conditions. A probable reason for this limitation is that the relative evaporation equation of the original GG model was empirically derived from 158 sites under wet environments in Canada. Thus, the complementary relationship in the GG model still needs improvements under dry conditions. The purpose of this study is, therefore, to extend the modified GG model of Anayah & Kaluarachchi (2014) to propose refinements to the relative evaporation equation in the original GG model to better predict regional  $E_T$ , especially under dry conditions and different land cover conditions. In addressing this goal, this work is still committed to use minimal data such as meteorological data and other readily accessible information with no local calibration.

Other classical approaches for estimating long-term  $E_T$  assume that evaporation is controlled by the availability of both energy and water (Pike 1964; Budyko 1974). For example, the Budyko hypothesis (1974) and the corresponding Budyko curve has been broadly used for estimating annual  $E_T$  as a function of the ratio of  $E_P$  to precipitation. Usually, potential evapotranspiration ( $E_P$ ) which measures the availability of energy and precipitation is a measure of availability of water. According to the Budyko hypothesis (1974), actual evapotranspiration in humid regions is controlled by potential evapotranspiration, while in arid regions, it is controlled by precipitation. However, the Budyko hypothesis (1974) makes no attempt to consider the impact of land surface characteristics such as vegetation cover. Later, other authors attempted to incorporate these characteristics into the Budyko hypothesis (1974). Examples of such widely used studies are Fu (1981) and Choudhury (1999). Choudhury (1999) developed an empirical equation by introducing the water equivalent of annual net radiation and an adjustable parameter which was estimated from field observations at eight locations with different vegetation types. Fu (1981) developed differential forms of the Budyko (1974) hypothesis through a dimensional analysis and

introduced a single parameter that determines the shape of the Budyko curve. This parameter can be calibrated from local data and represents land surface conditions such as vegetation cover, soil properties, and topography (Yang *et al.* 2006). This also supports the Penman hypothesis (1948) that  $E_T$  is proportional to  $E_P$ . Furthermore, Yang *et al.* (2008) derived the corresponding equivalence of Fu (1981) and Choudhury (1999) equations. While these expressions were not identical, their numerical values are the same. Thereafter, several studies used land surface characteristics including vegetation, soil types, and topography in the Budyko hypothesis using the work of Choudhury (1999) and Fu (1981) (Zhang *et al.* 2001, 2004; Yang *et al.* 2006, 2007, 2009; Li *et al.* 2013).

According to Zhang *et al.* (2004), the Fu equation can be restated that any change in evapotranspiration is a function of potential evapotranspiration and precipitation when precipitation is the only source of water. When there is no precipitation, evapotranspiration becomes zero and the atmospheric conditions are dry allowing potential evapotranspiration to reach the maximum. As precipitation increases, evapotranspiration increases and the atmosphere becomes cooler allowing potential evapotranspiration to decrease. This statement is similar to the complementary relationship introduced by Bouchet (1963). Yang *et al.* (2006) examined the complementary relationship using the long-term water balance data from 108 dry regions in China, and attempted to explain the consistency between the Budyko hypothesis and Bouchet hypothesis.

Recently, Li *et al.* (2013) focused on the vegetation impact and examined the conditions under which the vegetation index plays a major role in controlling the parameter  $\omega$  which represents the land surface characteristics and climate seasonality, and they proposed a simple process to estimate  $\omega$  using remote sensing vegetation information. Using data from 26 major global river basins, the basin-specific  $\omega$  was found to be a linear relationship with the long-term average annual vegetation cover. Vegetation cover is derived from the normalized difference vegetation index (NDVI). As a result, the new parameterization of  $\omega$  reduces the root mean square error ( $E_{RMS}$ ) by approximately 40% compared to the original Budyko framework.

As discussed earlier, the Budyko frameworks provide an opportunity to consider land surface characteristics,

especially the vegetation cover to improve  $E_T$  prediction. In this work, we proposed to upgrade the modified GG model of Anayah & Kaluarachchi (2014) to better predict ET under dry conditions using the Budyko framework. As mentioned before, one possible reason for poor performance of the original GG model is the use of data from wet regions of Canada, thus the GG model does not properly capture the prevailing dry conditions in arid regions. This work will use the approach in line with the earlier studies of Yang *et al.* (2006) and Zhang *et al.* (2004).

## METHODOLOGY AND DATA

### Methodology

#### Modified GG model

Anayah & Kaluarachchi (2014) developed their universal model using a three-step approach. First, they evaluated the original complementary methods under a variety of physical and climate conditions and developed 39 different model combinations. Second, three models' variations were identified based on performance compared to observed data from a set of global sites. Third, a statistical analysis was conducted to contrast and compare the three models to identify the best. The results showed that average  $E_{RMS}$ , mean absolute bias, and  $R^2$  across the 34 global sites were 20.6 mm/month, 10.6 mm/month, and 0.64, respectively. More importantly, the performance of this modified GG model increased partly due to the use of the Priestley & Taylor (1972) equation shown in Equation (2) to calculate  $E_W$  instead of the Penman (1948) equation.

$$E_W = \alpha \frac{\Delta}{\gamma + \Delta} (R_n - G_{soil}) \quad (2)$$

where  $E_W$  is in mm/d,  $\alpha$  is a coefficient equal to 1.28,  $R_n$  is net radiation (mm/d),  $\gamma$  is the psychrometric constant (kPa/°C),  $\Delta$  is the rate of change of saturation vapor pressure with temperature (kPa/°C), and  $G_{soil}$  is soil heat flux density (mm/d).

Also, two parameters were considered similar to the original GG (Granger & Gray 1989): relative drying power

( $D$ ) and relative evaporation ( $G$ ).  $D$  and  $G$  are described in Equations (3) and (5), respectively:

$$D = \frac{E_a}{E_a + (R_n - G_{soil})} \quad (3)$$

where  $E_a$  is drying power of air (mm/d) given in Equation (4):

$$E_a = 0.35(1 + 0.54U)[(e_s - e_a)] \quad (4)$$

where  $U$  is wind speed at 2 m above ground level (m/s) that needs adjustments and conducted using the procedure described by Allen *et al.* (1998),  $e_s$  is saturation vapor pressure (mmHg),  $e_a$  is vapor pressure of air (mmHg).

$$G = \frac{E_T}{E_P} = \frac{1}{c_1 + c_2 e^{c_3 D}} \quad (5)$$

where  $c_1 = 1.0$ ,  $c_2 = 0.028$ , and  $c_3 = 8.045$ . The effect of  $G_{soil}$  is negligible compared to  $R_n$  when calculated at monthly or higher timescale (e.g., Hobbins *et al.* 2001).

Solving Equation (5) for  $E_P$  and substituting in Equation (1), the modified GG model is given in Equation (6):

$$E_T = \frac{2G}{G + 1} E_W \quad (6)$$

Therefore, the modified GG model of Anayah & Kaluarachchi (2014) can estimate  $E_T$  directly without calculating  $E_P$ .

### Budyko framework

Fu (1981) proposed the differential forms of the Budyko framework through a dimensional analysis. The corresponding analytical solution of the Budyko framework is given in Equation (7) or (8):

$$\frac{E_T}{P} = 1 + \frac{E_P}{P} - \left[ 1 + \left( \frac{E_P}{P} \right)^\sigma \right]^{1/\sigma} \quad (7)$$

$$\frac{E_T}{E_P} = 1 + \frac{P}{E_P} - \left[ 1 + \left( \frac{P}{E_P} \right)^\sigma \right]^{1/\sigma} \quad (8)$$

where  $P$  is precipitation (mm) and  $E_P$  is estimated using the Priestly and Taylor equation (1972). Parameter  $\omega$  is a constant and represents the land surface conditions of the basin, especially the vegetation cover (Li *et al.* 2013). Li *et al.* (2013) showed that  $\omega$  is linearly correlated with the long-term average annual vegetation cover and a model using NDVI can improve the estimation of  $E_T$ . In that study, vegetation cover defined by  $M$  is calculated as (Yang *et al.* 2009):

$$M = \frac{NDVI - NDVI_{min}}{NDVI_{max} - NDVI_{min}} \quad (9)$$

where  $NDVI_{min}$  is minimum NDVI and  $NDVI_{max}$  is maximum NDVI. The values of  $NDVI_{min}$  and  $NDVI_{max}$  are constants at 0.05 and 0.8, respectively (Yang *et al.* 2009). Then, an optimal  $\omega$  value for the basin can be derived through a curve fitting procedure that minimizes the mean squared error between the measured and predicted

evaporation ratio (Li *et al.* 2013). The objective function used to find optimal  $\omega$  is:

$$Obj_{\omega} = \min \sum_i \left\{ \frac{(E_T)_i}{P_i} - \left\{ 1 + \frac{(E_P)_i}{P_i} - \left[ 1 + \left( \frac{(E_P)_i}{P_i} \right)^{\omega} \right]^{1/\omega} \right\} \right\}^2 \quad (10)$$

where  $i$  is year. Li *et al.* (2013) proposed parameterization that is simply a linear regression between optimal  $\omega$  and long-term average  $M$  given as:

$$\omega = a \times M + b \quad (11)$$

where  $a$  and  $b$  are constants that are found for each site.

### Proposed GG model refinements

Figure 1 illustrates a schematic of the complementary relationship and the Budyko framework. Figure 1(a)

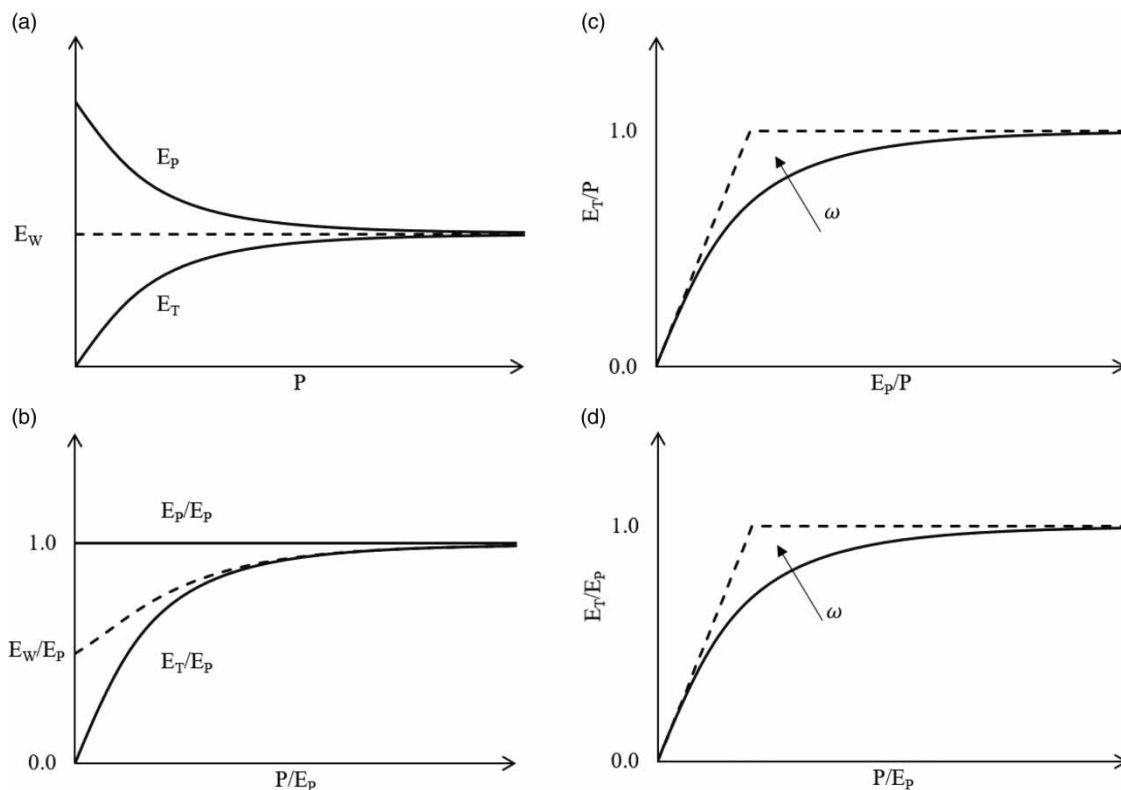


**Figure 1** | A schematic of the complementary relationship and the Fu equation: (a) original complementary relationship of Bouchet (1963), (b) updated complementary relationship with division by  $E_P$ , (c) Budyko hypothesis on the basis of Equation (7), and (d) Budyko hypothesis on the basis of Equation (8).

shows the original complementary relationship proposed by Bouchet (1963) which translates to Figure 1(b) if all variables are divided by  $E_p$ . Figure 1(c) is the original curve describing the Budyko hypothesis on the basis of Equation (7), where  $\varpi$  is the curve shape factor of the Fu equation. Figure 1(d) shows the other form of the Fu equation, as given in Equation (8). Comparing Figure 1(b) and 1(d), it can be concluded that the complementary relationship is consistent with the Budyko hypothesis through the Fu equation.

In the modified GG model (Anayah & Kaluarachchi 2014), the ratio of  $E_T$  to  $E_p$  is defined as relative evaporation ( $G$ ), as shown in Equation (5). Parameter  $G$  was empirically derived using limited data from wet environments in western Canada (Granger & Gray 1989). As discussed earlier, this bias towards wet region data may be the reason for relatively poor predictions with the GG model under dry conditions. In order to improve the  $E_T$  predictions of the modified GG model (Anayah & Kaluarachchi 2014), given by Equation (6), parameter  $G$  needs improvements. If this ratio can be improved and used appropriately in the modified GG model with the Fu equation, it would bring about the Budyko framework which works well in dry conditions and maintains the complementary relationship. For this purpose, we used the theoretical framework of the Fu equation developed by Li *et al.* (2013) on the basis of the work of Yang *et al.* (2006) and Zhang *et al.* (2004). Equation (12) shows the Fu equation where the ratio of  $E_T/E_p$  is now defined as  $G_{new}$ :

$$G_{new} = \frac{E_T}{E_p} = 1 + \frac{P}{E_p} - \left[ 1 + \left( \frac{P}{E_p} \right)^\varpi \right]^{1/\varpi} \quad (12)$$

Note  $G_{new}$  in Equation (12) is the new (updated) definition of relative evaporation,  $G$ , which includes the Budyko hypothesis and vegetation index. To estimate  $G_{new}$ ,  $E_p$  is required and can be estimated using the equation from Penman (1948), given in Equation (13):

$$E_p = \frac{\Delta}{\gamma + \Delta} (R_n - G_{soil}) + \frac{\gamma}{\gamma + \Delta} E_a \quad (13)$$

Having found  $G_{new}$  from Equation (12) and estimating  $E_w$  from Equation (2), we can estimate  $E_T$  of the proposed

model from Equation (14):

$$E_T = \frac{2G_{new}}{G_{new} + 1} E_w \quad (14)$$

Hereafter, this proposed model will be referred to as the GG-NDVI model. Essentially, GG-NDVI is a combination of the complementary relationship through the modified GG model and the Budyko hypothesis that uses NDVI to describe the vegetation cover.

## Data

The complementary method requires meteorological data for estimating  $E_T$  and these include temperature, pressure or elevation, net radiation, and wind speed. As seen from Table 1, the GG-NDVI model requires two additional data strings, precipitation and NDVI, compared to the modified GG model proposed by Anayah & Kaluarachchi (2014). FLUXNET is a global network of micrometeorological tower sites. A flux tower uses the EC method to measure ecosystem-scale mass and energy fluxes. This study proposes to use data from AmeriFlux EC tower sites in the USA, a part of FLUXNET, because the US sites have a wide variety of climatic and physical conditions and land cover, especially in dry regions. At present, there are over 110 sites where data are collected at 30-minute intervals. In some cases, data are not available at monthly intervals and for such instances mean monthly data were aggregated

**Table 1** | Required meteorological data for different  $E_T$  estimation methods including the GG-NDVI model proposed in this study

	CRAE	Modified GG <sup>a</sup>	GG-NDVI <sup>b</sup>	ASCE <sup>c</sup>
Temperature (min, max)	●	●	●	●
Pressure (or elevation)	●	●	●	●
Net radiation	●	●	●	●
Wind speed		●	●	●
Precipitation			●	
NDVI			●	
$C_n, C_d^d$				●

<sup>a</sup>From Anayah & Kaluarachchi (2014).

<sup>b</sup>Proposed in this work.

<sup>c</sup>From Allen *et al.* (2005).

<sup>d</sup> $C_n$  and  $C_d$  are constants that change with reference crop and time step.

from 30-minute time-scale that are available from Level 2 data of AmeriFlux. This study selected 75 sites with less than 50% missing data and the selected sites are shown in Figure 2. These data were obtained from the Oak Ridge National Laboratory's AmeriFlux website (<http://ameriflux.ornl.gov/>, last accessed: November 2015). These sites provide ten land cover types and a wide range of climates. The land cover types developed by the International Geosphere-Biosphere Programme (IGBP) include evergreen needleleaf forests (ENF), evergreen broadleaf forests (EBF), deciduous broadleaf forests (DBF), mixed forests (MF), closed shrublands (CSH), open shrublands (OSH), woody savannas (WSA), grasslands (GRA), permanent wetlands (WET), and croplands (CRO). Table 2 shows that the largest portion of land cover in the dry sites is GRA at 31% and the wet sites have ENF at 44%. The observed  $E_T$  to validate the proposed model was calculated from measured latent heat flux (LE) data from EC towers using the equation  $E_T = LE/\lambda$  where  $\lambda$  is latent heat of vaporization (J/kg).

To classify the climatic conditions, the ratio of  $P/E_p$ , which is called the aridity index of the United Nations

Environment Program (AIU) was used (Barrow 1992). AIU divides climatic conditions into six classes: hyper-arid regimes ( $AIU < 0.05$ ), arid ( $0.05 \leq AIU < 0.20$ ), semi-arid ( $0.20 \leq AIU < 0.50$ ), dry sub-humid ( $0.50 \leq AIU < 0.65$ ), wet sub-humid ( $0.65 \leq AIU < 0.75$ ), and humid ( $AIU \geq 0.75$ ). Similar to Anayah & Kaluarachchi (2014), this work simplified the climatic class definitions into two classes, simply combining hyper-arid regimes, arid, semi-arid, and dry sub-humid to define the dry class and wet sub-humid and humid as the wet class. Using this simplified and updated definition, 36 sites fall to the dry class and 39 sites fall to the wet class. Mean AIU of the dry and wet sites are 0.41 and 0.92, respectively. The details of AIU values and additional details of 75 sites are given in Table 3.

There are two methods available to compute net radiation: Morton (1983) and Allen *et al.* (2005). Morton (1983) proposed net radiation for soil-plant surfaces at an equilibrium temperature that is derived from the solution to the water vapor transfer and energy-balance equations under a small moist surface. On the other hand, Allen *et al.* (2005) predicted net radiation from observed short wave radiation,

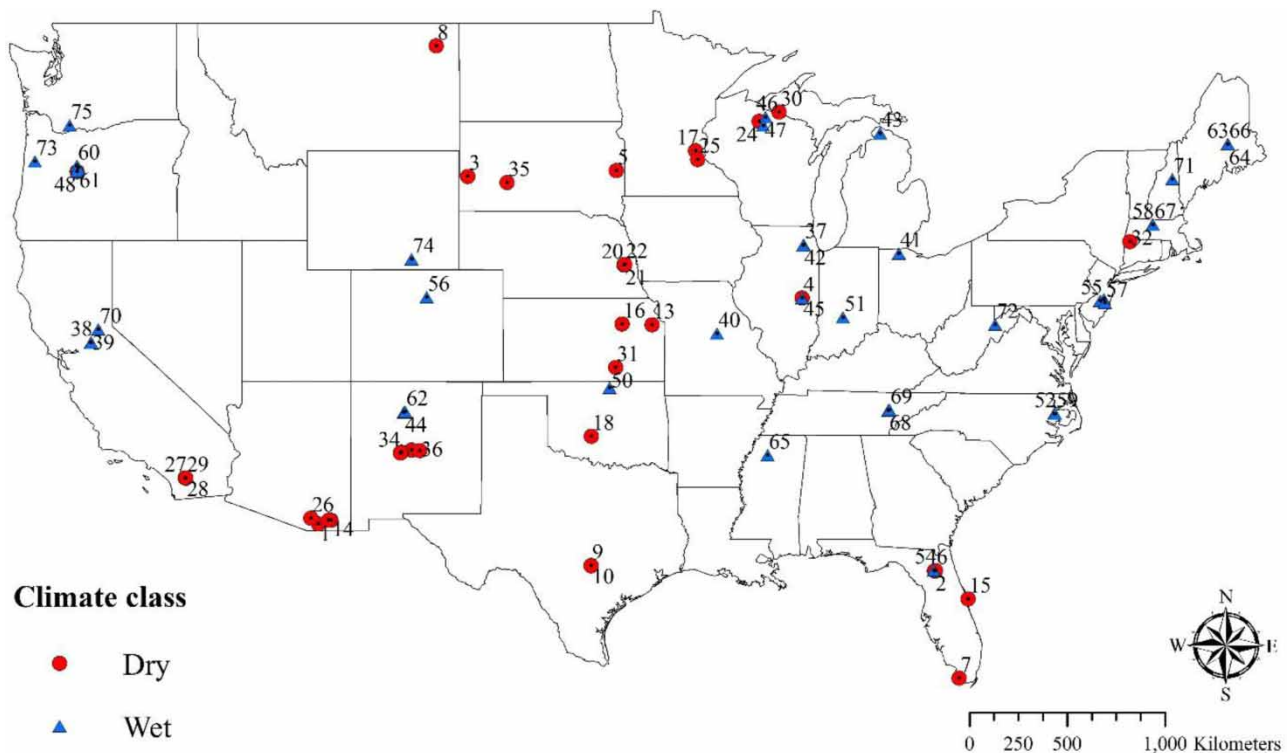


Figure 2 | Locations of 75 AmeriFlux EC towers used in this study.

**Table 2** | Land cover class distribution of the 75 EC sites from the AmeriFlux database used in this study with IGBP (International Geosphere-Biosphere Program)

IGBP Land cover class	Dry (36 sites)	Wet (39 sites)
Evergreen needleleaf forests (ENF)	11% (4 sites)	44% (17 sites)
Evergreen broadleaf forests (EBF)	3% (1 site)	–
Deciduous broadleaf forests (DBF)	–	28% (11 sites)
Mixed forests (MF)	8% (3 sites)	3% (1 site)
Closed shrublands (CSH)	14% (5 sites)	5% (2 sites)
Open shrublands (OSH)	11% (4 sites)	–
Woody savannas (WSA)	6% (2 sites)	3% (1 site)
Grasslands (GRA)	31% (11 sites)	10% (4 sites)
Permanent wetlands (WET)	3% (1 site)	–
Croplands (CRO)	14% (5 sites)	8% (3 sites)

vapor pressure, and air temperature; this method is routine and generally accurate. Anayah & Kaluarachchi (2014) found that the method described by Allen *et al.* (2005) is better than that of Morton (1983). In this study, we used mean of daily maximum and minimum temperatures to define mean daily air temperature in order to standardize air temperature. For NDVI, we retrieved 16-Day L3 Global 250 m SIN Grid (<http://daac.ornl.gov/MODIS/modis.shtml>) of MODIS. Generally, NDVI values are between  $-1$  and  $1$ , with values  $>0.5$  indicating dense vegetation and  $<0$  indicating water surface. The NDVI values of this study varied between  $0.18$  and  $0.76$ . The mean NDVI is  $0.44$  for dry sites and  $0.60$  for wet sites and the distribution of NDVI is shown in Figure 3(a). The average annual precipitation varied from  $249$  mm to  $1,312$  mm with a mean of  $703.1$  mm for dry sites and from  $494$  mm to  $2,452$  mm with a mean of  $1,033.3$  mm for wet sites and the distribution of precipitation is shown in Figure 3(b). Data were available from 1995 to 2013. The shortest data available period is 3 years at one of the sites and the longest period is 19 years.

## RESULTS AND DISCUSSION

This study used two scenarios to evaluate the performance of the proposed GG-NDVI model. In Scenario 1, the modified GG model of Anayah & Kaluarachchi (2014) is used for direct comparison and this scenario used all 75 AmeriFlux

sites (36 dry and 39 wet sites). In Scenario 2, the original GG model described by Han *et al.* (2012) (also called the normalized complementary method) and the CRAE method of Morton (1983) are used for comparison. Scenario 2 used only 59 sites (29 dry and 30 wet sites) since only these 59 sites have incident global radiation data required by the CRAE model.

### Scenario 1: comparison with the modified GG model

Table 4 shows the comparison of results between the proposed GG-NDVI and the modified GG models. The GG-NDVI model reduces the mean  $E_{RMS}$  by about 32% and 15% for dry and wet sites, respectively. In the dry sites, the GG-NDVI model showed higher maximum  $E_{RMS}$  values compared to the modified GG model but the mean is much lower at  $13.9$  mm/month compared to  $20.5$  mm/month. On the other hand, the wet class values are comparable. Although the maximum increased with GG-NDVI for the dry sites, the lower mean value indicates more occurrence of lower values with GG-NDVI. Figure 4 confirms this observation where the occurrences of less than  $10$  mm/month is more frequent than the modified GG model. Similar results are seen with the wet sites as well, except, even higher occurrences of low  $E_{RMS}$  values. The results also show that  $E_T$  estimates of both models improve with wetness similar to other previous studies discussed earlier.

The major difference between the two models is the use of vegetation to estimate  $E_T$  in the GG-NDVI model. To assess the contribution of NDVI on GG-NDVI, the variation of NDVI with  $E_{RMS}$  was studied but is not shown here. The  $E_{RMS}$  distribution of the GG-NDVI model that uses NDVI is consistently below  $25$  mm/month with 92% (33 sites) of the dry sites compared to 58% (21 sites) with the modified GG model that does not account for NDVI.

Most dry sites used in this work have hot summer and warm winter seasons with low vegetation density (low NDVI). For instance, the mean annual temperature at the Freeman Ranch in Texas is  $20$  °C and there is significant precipitation during summer. The minimum, maximum, and mean  $E_{RMS}$  of the GG-NDVI model were  $0.01$ ,  $48.4$ , and  $14.0$  mm/month, respectively. Figure 5 shows a comparison of monthly  $E_T$  of the modified GG and GG-NDVI models

**Table 3** | Details of the 75 AmeriFlux EC sites selected for this study; P is mean annual precipitation, T is mean annual temperature, AIU is aridity index of UNEP, and EL is elevation

#	Site ID	T (°C)	P (mm)	AIU	EL. (m)	#	Site ID	T (°C)	P (mm)	AIU	EL. (m)
<b>Dry</b>											
1	US-Seg	13.4	250	0.15	1,622	19	US-Ne3	10.1	784	0.45	363
2	US-Ses	17.7	250	0.16	1,593	20	US-Kon	12.8	867	0.46	330
3	US-Ctn	9.7	278	0.16	744	21	US-Ne2	10.1	789	0.46	362
4	US-Wjs	12.1	249	0.16	1,926	22	US-Ivo	-8.3	304	0.47	568
5	US-Whs	17.1	355	0.20	1,372	23	US-Wlr	13.5	881	0.49	408
6	US-FPe	5.5	335	0.22	364	24	US-PFa	4.3	823	0.49	470
7	US-SRM	17.9	380	0.22	1,120	25	US-Blk	6.2	574	0.50	1,718
8	US-Wkg	15.6	407	0.24	1,531	26	US-Syv	3.8	826	0.50	540
9	US-Mpj	10.4	330	0.25	2,138	27	US-FR2	19.5	864	0.51	272
10	US-Aud	14.9	438	0.26	1,469	28	US-KUT	8.0	701	0.52	301
11	US-SP1	20.1	1,310	0.26	50	29	US-FR3	19.6	869	0.52	232
12	US-SO4	14.7	484	0.34	1,429	30	US-Skr	23.8	1,259	0.53	0
13	US-SO3	13.3	576	0.37	1,429	31	US-KFS	12.0	1,014	0.58	310
14	US-SO2	13.6	553	0.39	1,394	32	US-Ro1	6.9	806	0.60	260
15	US-Bkg	6.0	586	0.41	510	33	US-Bo1	11.0	991	0.61	219
16	US-LWW	16.1	805	0.43	365	34	US-Me3	7.1	719	0.61	1,005
17	US-GMF	6.1	1,259	0.44	380	35	US-KS2	21.7	1,294	0.64	3
18	US-Ne1	10.1	790	0.45	361	36	US-SP3	20.3	1,312	0.64	50
<b>Wet</b>											
1	US-IB1	9.0	929	0.65	227	21	US-Ced	11.0	1,138	0.83	58
2	US-Ton	15.8	559	0.65	177	22	US-LPH	7.0	1,071	0.87	378
3	US-Var	15.8	559	0.65	129	23	US-NC2	16.0	1,294	0.89	12
4	US-Moz	12.0	986	0.65	220	24	US-Me4	8.0	1,039	0.9	922
5	US-Oho	9.0	843	0.66	230	25	US-Me5	6.0	591	0.91	1,188
6	US-IB2	9.0	930	0.66	227	26	US-Vcm	6.0	646	0.91	3,003
7	US-UMB	6.0	803	0.68	234	27	US-Ho2	5.0	1,064	0.93	91
8	US-Vcp	7.0	693	0.68	2,542	28	US-Ho1	5.0	1,070	0.94	60
9	US-Bo2	11.0	991	0.69	219	29	US-Goo	16.0	1,426	0.94	87
10	US-Los	4.0	828	0.69	480	30	US-Ho3	5.0	1,072	0.94	61
11	US-WCr	4.0	787	0.71	520	31	US-Ha1	7.0	1,071	0.97	340
12	US-Me6	7.6	494	0.71	998	32	US-ChR	14.0	1,359	1.00	286
13	US-Me2	6.3	523	0.71	1,253	33	US-WBW	14.0	1,372	1.09	283
14	US-Pon	14.9	866	0.74	310	34	US-Blo	11.0	1,226	1.06	1,315
15	US-MMS	11.0	1,032	0.75	275	35	US-Bar	6.0	1,246	1.14	272
16	US-NC1	16.0	1,282	0.81	5	36	US-CaV	8.0	1,317	1.15	994
17	US-Dix	11.0	1,127	0.81	48	37	US-MRf	10.0	1,820	1.75	263
18	US-SP2	20.0	1,314	0.81	43	38	US-GLE	1.0	525	2.08	3,190
19	US-Slt	11.0	1,152	0.82	30	39	US-Wrc	9.0	2,452	2.31	371
20	US-NR1	2.0	800	0.82	3,050						

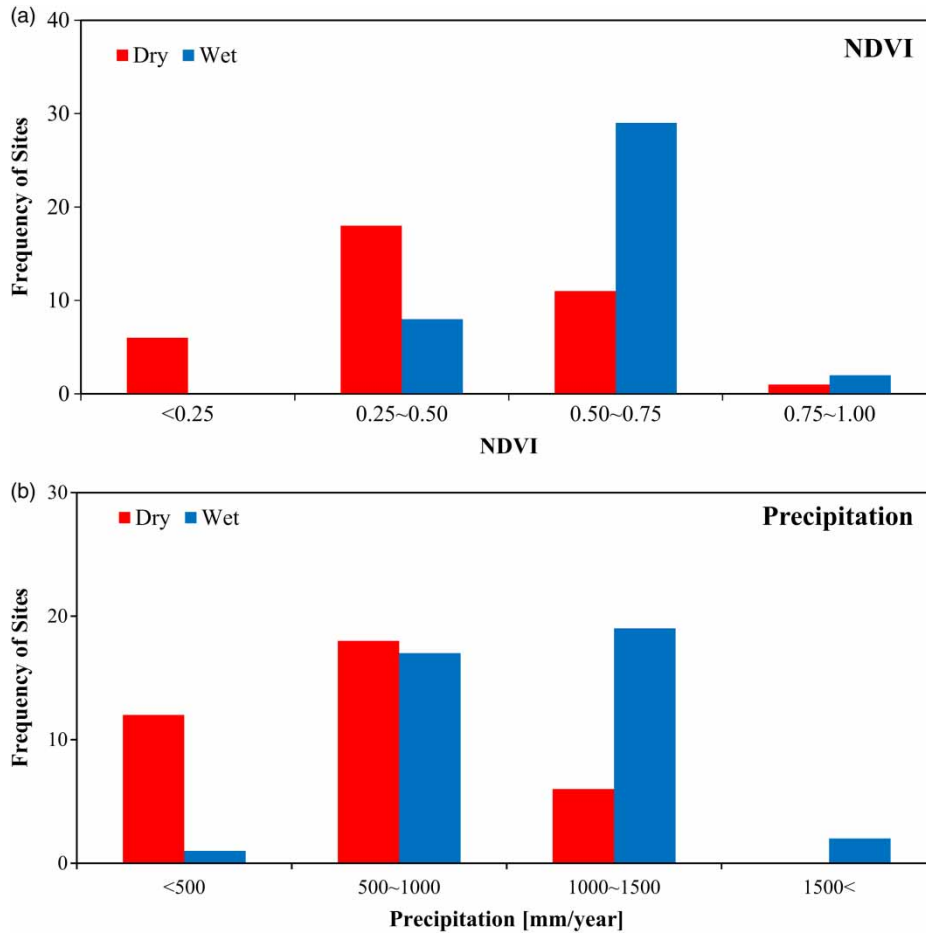


**Figure 3** | Distribution of (a) NDVI and (b) precipitation for dry and wet sites.

**Table 4** | Comparison of performance using  $E_{RMS}$  (mm/month) of GG-NDVI compared to other models described in Scenarios 1 and 2

Method	Dry sites			Wet sites		
	Min	Mean	Max	Min	Mean	Max
Scenario 1: All 75 sites (36 dry and 39 wet sites)						
Modified GG	0.3	20.5	42.7	0.6	12.5	36.0
GG-NDVI	0.4	13.9	56.6	0.3	10.7	31.5
Scenario 2: 59 sites only (29 dry and 30 wet sites)						
Modified GG	1.7	21.4	42.7	0.6	12.9	36.0
GG-NDVI	0.4	14.7	56.6	0.3	11.6	28.5
CRAE	0.5	18.9	53.9	0.8	22.3	62.3
GG	0.1	32.3	75.1	1.1	19.6	60.1

with observed  $E_T$  from 2005 to 2008. The mean  $E_{RMS}$  of the modified GG model is 20.6 mm/month. While the modified GG model showed a regular and periodic performance and

significant deviation from observed  $E_T$ , the pattern of GG-NDVI is similar to the observed values. We observe similar results at the Goodwin Creek site in Mississippi, as shown in Figure 6. A reasonable conclusion would be that GG-NDVI is improved by using the vegetation cover information in the model. On the other hand, the method that uses only climatic data seems incomplete in estimating  $E_T$ . This conclusion is supported by Bethenod *et al.* (2000) and Potter *et al.* (2005). Even under low vegetation cover (low NDVI) conditions, plant transpiration accounts for most  $E_T$  from 20% to as much as 80%. Moreover, hot summer and warm winter months are producing high fluctuation of plant transpiration and, therefore, high fluctuation of  $E_T$  (Hsiao & Henderson 1985). In this regard, the GG-NDVI model can be expected to be more accurate than the modified GG model due to the use of NDVI to better

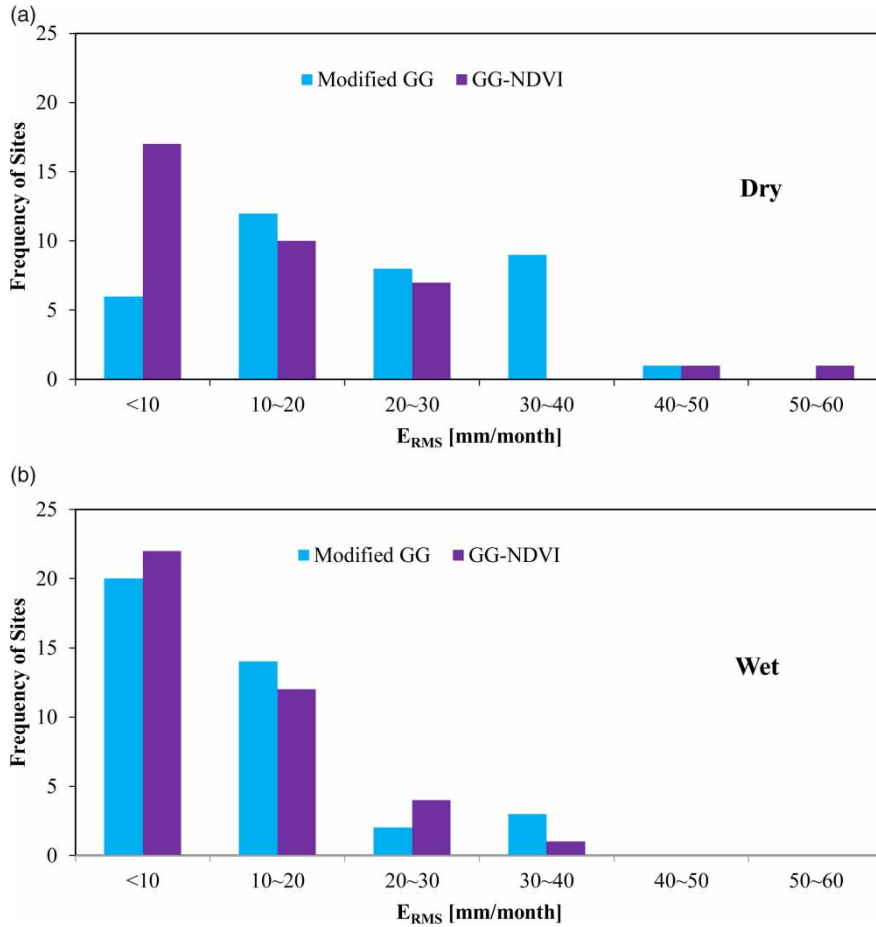


**Figure 4** | Histogram of  $E_{RMS}$  of GG-NDVI and the modified GG models for (a) dry and (b) wet sites.

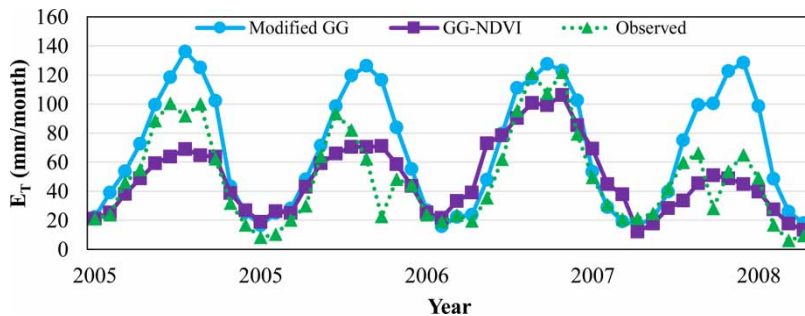


**Figure 5** | Comparison of monthly  $E_T$  distribution and observed  $E_T$  at Freeman Ranch in Texas for the period 2005–2008.

represent plant transpiration, whereas meteorological data alone may not be sufficient to estimate  $E_T$  under dry conditions.

Meanwhile, the simulated patterns of  $E_T$  from the modified GG model may be representing the principles of

the complementary relationship. First, the complementary relationship assumes a homogeneous surface layer that assumes the mixing of the effects of surface environmental discontinuities. When surface discontinuities are prevalent, such as in the western United States where vegetation is

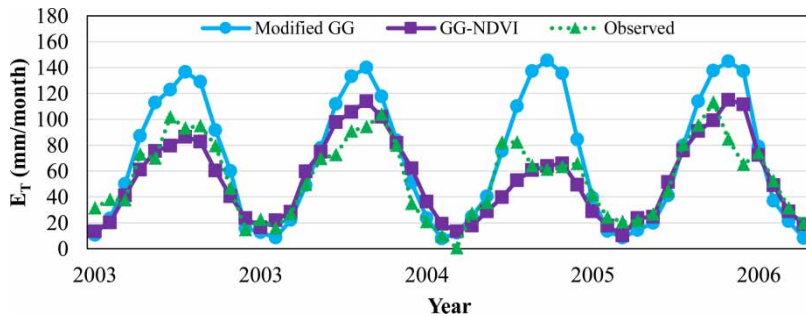


**Figure 6** | Comparison of monthly  $E_T$  distribution and observed  $E_T$  at Goodwin Creek in Mississippi for the period 2003–2006.

less flourishing than other regions, this assumption may not be valid. Second, given the heterogeneity of surface conditions, the approaches used in identifying and calculating the various input data may not be perfect in the modified GG model. For these reasons, the modified GG model probably showed a regular and periodic performance in estimated  $E_T$  and therefore the differences with observed  $E_T$ .

Among the results of GG-NDVI, it should be noted that there are two sites with relatively large  $E_{RMS}$  (higher than 40 mm/month). One is Brookings in South Dakota and the other is Florida Shark River in Florida. The IGBP land cover class of Brookings site is grassland which is representative of the north central United States. The

mean annual precipitation from 2005 to 2009 is 586 mm at this site. The mean NDVI of Brookings is 0.41 and this site has a large seasonal vegetation cover, as shown in Figure 7. Although not shown here, the Florida Shark River site has a mean annual precipitation of 1,259 mm from 2007 to 2010 and the annual rainfall is high during the summer season. This site has a high dense vegetation cover with NDVI of 0.75.

A possible reason for high  $E_{RMS}$  could be that NDVI is not the best index to represent the vegetation cover in this site given the large seasonal variation and dense vegetation cover. According to [Pettorelli et al. \(2005\)](#), the soil-adjusted vegetation index (SAVI) is recommended instead of NDVI for areas with leaf area index (LAI) less than 3. It should

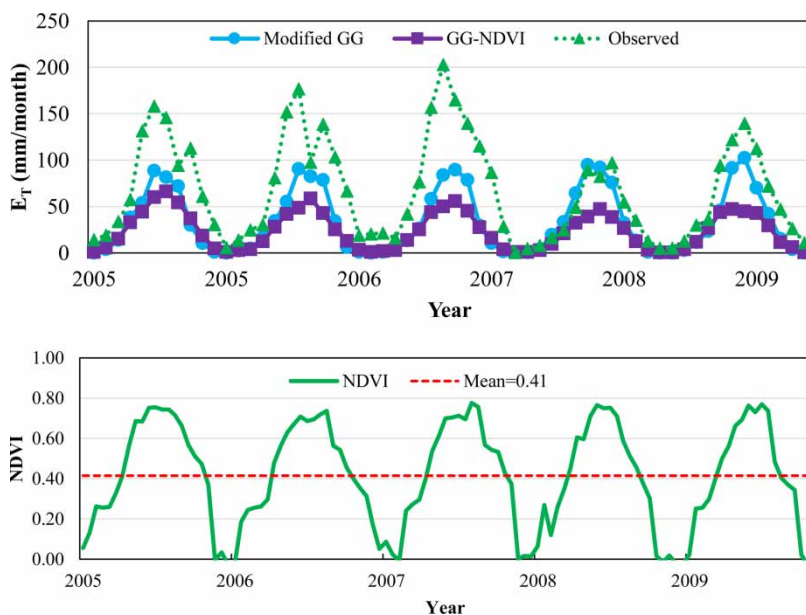


**Figure 7** | Comparisons of monthly  $E_T$  and observed  $E_T$  and corresponding time-series of NDVI at the Brookings site in South Dakota.

be noted that the LAI of Brookings and Florida sites is 2.5 and 2.9, respectively. However, a limitation of SAVI is it requires soil brightness correction with local calibration (Huete 1988). Mu *et al.* (2007) modified their algorithm to include vapor pressure deficit, minimum air temperature, and LAI, and replaced NDVI with the enhanced vegetation index (EVI) to represent dense vegetation conditions. Prior studies have also demonstrated that NDVI is insufficient to account for transpiration under dense vegetation cover conditions (Pettorelli *et al.* 2005; Yuan *et al.* 2010; Mu *et al.* 2011). For these reasons, the modified GG model showed better performance than GG-NDVI at both sites;  $E_{RMS}$  of the modified GG for the Brookings site is 33 mm/month compared to 44 mm/month with GG-NDVI and 15 mm/month for the Florida site compared to 56 mm/month with GG-NDVI.

These results suggest that models using the complementary relationship may not predict  $E_T$  accurately as the vegetation cover becomes dense. Beyond a given level of vegetation cover density and seasonality, NDVI is not capturing plant transpiration correctly, as seen with the Florida Shark River site. In essence, these results suggest that a different vegetation index, such as EVI, may be needed to better predict  $E_T$ .

## Scenario 2: comparison with other complementary methods

The CRAE method is considered to be simple, practical and a reliable method to estimate monthly  $E_T$  (Hobbins *et al.* 2001). Han *et al.* (2012) developed the normalized complementary method which is based on the CRAE method. This study found that the method performed better than the AA model in predicting  $E_T$  under dry and wet conditions. However, the normalized complementary method was tested using only four sites with different land covers. Therefore, this study provides the opportunity to test both models, CRAE and GG models, compared to the proposed GG-NDVI model. This comparison used only 59 sites from the 75 sites due to the reason described earlier.

The results of the comparison are given in Table 4. Again, all models showed high maximum  $E_{RMS}$  values in dry sites in the order of more than 40 mm/month. However,

the GG-NDVI model showed the lowest mean  $E_{RMS}$  across all models at 14.7 mm/month for the dry and 11.6 mm/month for the wet sites. The modified GG model was the third best for mean values for the dry sites. The GG-NDVI model performed much better in the wet category too. The GG-NDVI model produced the lowest mean  $E_{RMS}$  for the dry sites and lowest mean and maximum  $E_{RMS}$  for the wet sites. The results in general indicate that GG-NDVI can perform well in the dry regions and even better in the wet sites. These results also confirm the observation of Xu & Singh (2005) that showed the estimation capability of  $E_T$  reduces with increased aridity.

The CRAE model assumes that the vapor transfer coefficient is independent of wind speed and this may lead to errors in calculating  $E_T$ . The complementary relationship-driven models do not directly use soil moisture information and hence may overestimate  $E_T$  as aridity increases (Xu & Singh 2005). This reason may cause decreased predictive power of these methods using the complementary method. To evaluate this concern, this study used the 59 sites and simulated  $E_T$  using the CRAE method, modified GG model of Anayah & Kaluarachchi (2014), original GG model, and the proposed GG-NDVI model. Figure 8 presents a comparison of the  $E_{RMS}$  distribution of these four models and the corresponding boxplots are shown in Figure 9. The results indicate better performance of the GG-NDVI model compared to the other models. For example, most values of  $E_{RMS}$  of the GG-NDVI model are at less than 20 mm/month interval. The number of less than 20 mm/month contributed 72% of the 29 dry sites in the GG-NDVI model in comparison with 48% with GG, 55% with CRAE, and 45% with the modified GG. Figure 9 shows that the GG-NDVI model has the lowest mean error across all four methods especially in the dry sites while maintaining a low range of  $E_{RMS}$  values.

GG-NDVI underestimates  $E_T$  in most dry sites during the rainy months. For example, the Audubon Research Ranch site in Arizona is considered dry with an annual precipitation of about 438 mm. About 70% of annual precipitation is present in the rainy months from July to September. In this period, the GG-NDVI model underestimated  $E_T$ , as shown in Figure 10. A possible explanation was mentioned by Budyko (1974) and Gerrits *et al.* (2009). They found that locations where monthly  $E_P$  and precipitation are out of

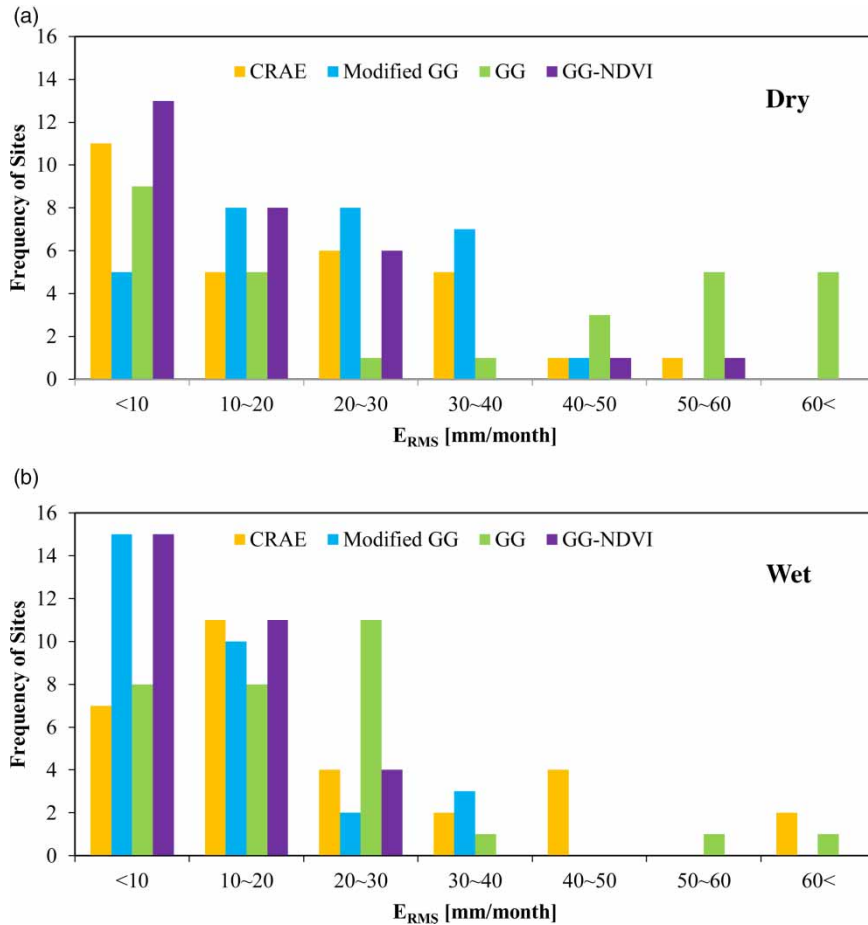


**Figure 8** | Histogram of  $E_{RMS}$  for GG-NDVI and other complementary methods. GG refers to the normalized complementary method of Han *et al.* (2012).

phase, for example in a dry site,  $E_T$  is generally underestimated. Similarly,  $E_T$  decreases with increasing  $E_P$  on the basis of the complementary relationship and  $E_P$  is overestimated in regions of decreasing moisture availability. According to Hobbins *et al.* (2001), a negative relationship between wind speed and  $E_P$  and the mean monthly values of wind speed are lowest in the summer months. Hence, higher  $E_P$  estimates and correspondingly lower  $E_T$  estimates should be expected for these summer months with higher precipitation.

Although not shown here, we plotted monthly  $E_{RMS}$  and precipitation to evaluate the relationship between model accuracy and wetness. The results showed a weak relationship for dry sites. Figure 11(a) shows the relationship between the correlation coefficient between precipitation and  $E_{RMS}$  versus mean annual precipitation. Results indicate

that GG-NDVI produce errors that increase in variability with increasing precipitation and this trend decreases with increasing precipitation based on the negative slope of least fit (dashed-line in Figure 11(a)). Accordingly, the R-square for this relationship from GG-NDVI across all 75 sites is 0.322. While this value is not high, it is still better than the results obtained from the CRAE and AA models by Hobbins *et al.* (2001) which were 0.148 and 0.314, respectively.

Figure 11(b) shows the relationship between the correlation coefficient between AIU and  $E_T$ , and AIU. The correlation coefficients for the wet sites are mostly negative and ranged from  $-0.68$  to  $-0.11$ . On the contrary, many dry sites have positive correlation coefficients. This implies that increasing AIU decreased  $E_T$  for most wet sites but increased for most dry sites. These trends are characteristics

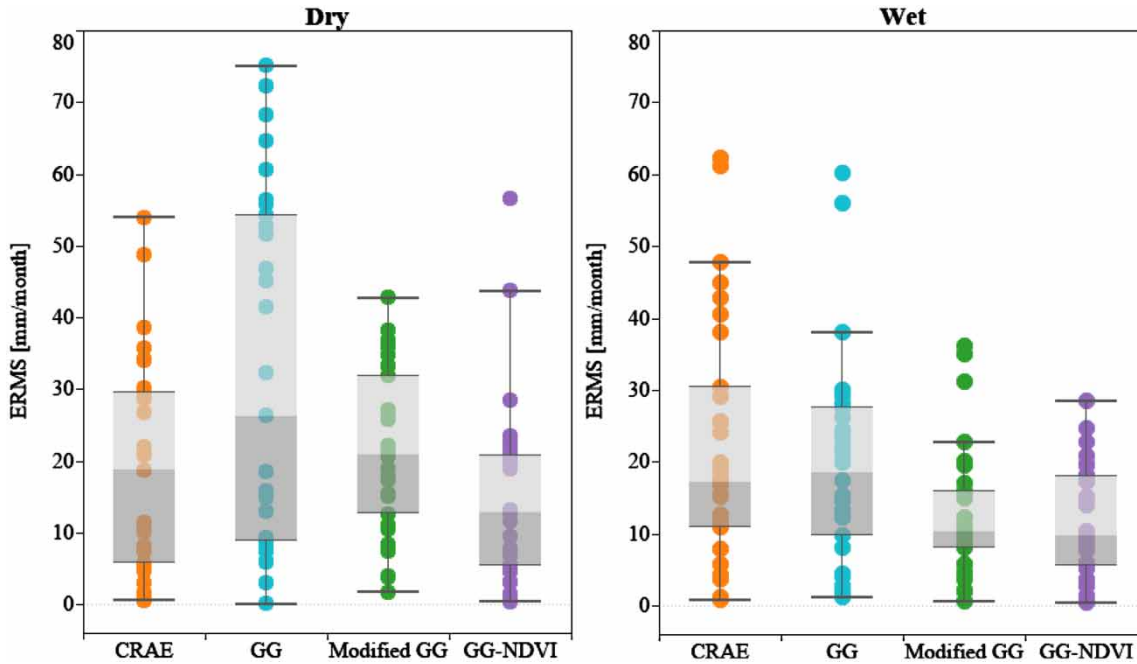


Figure 9 | Boxplots of  $E_{RMS}$  between different complementary methods of Scenario 2. GG refers to the normalized complementary method of Han et al. (2012).

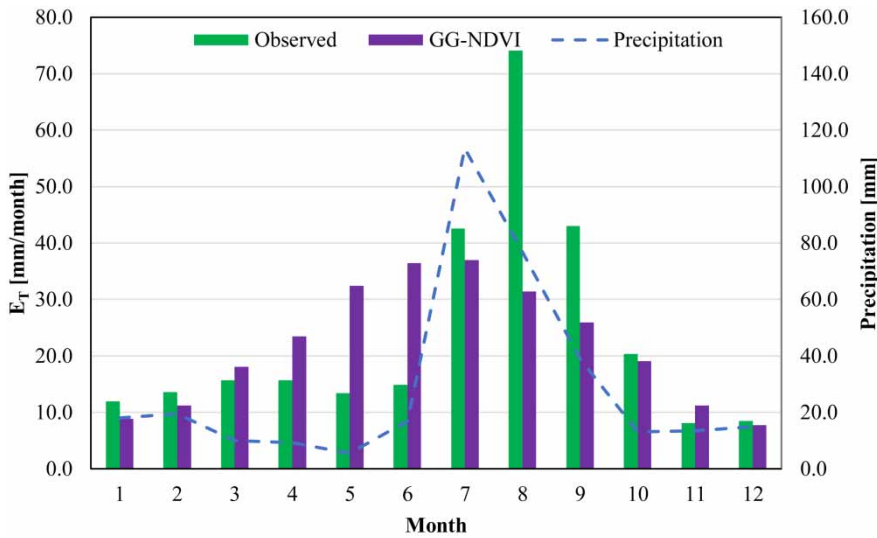


Figure 10 | Comparison of mean monthly  $E_T$  of GG-NDVI and observed values at the Audubon site in Arizona.

of the complementary relationship and have been observed by Roderick et al. (2009) and Han et al. (2014).

For a clear relationship between vegetation cover and  $E_T$ , Figure 12 displays the estimated  $E_T$  with NDVI for all 75 sites. In a linear regression analysis between both, NDVI explains 51% of the variance in the estimated  $E_T$  and similar observations have been made by Hsiao &

Henderson (1985), Bethenod et al. (2000), and Hsiao & Xu (2005).

**Comparison with other published studies**

Table 5 shows a comparison between the results of the proposed GG-NDVI model and the results from recently published

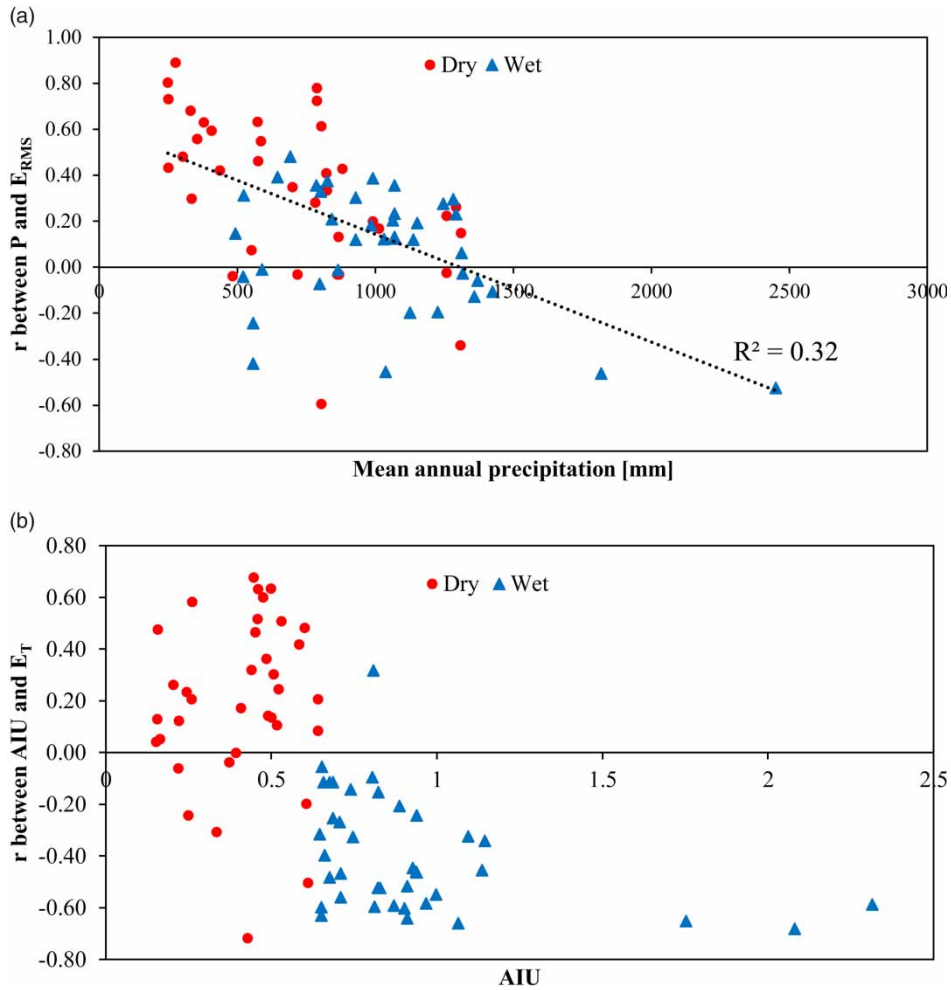


**Figure 11** | (a) Correlation coefficient between precipitation and  $E_{RMS}$  versus mean annual precipitation. (b) Correlation coefficient between AIU and  $E_T$  versus AIU.

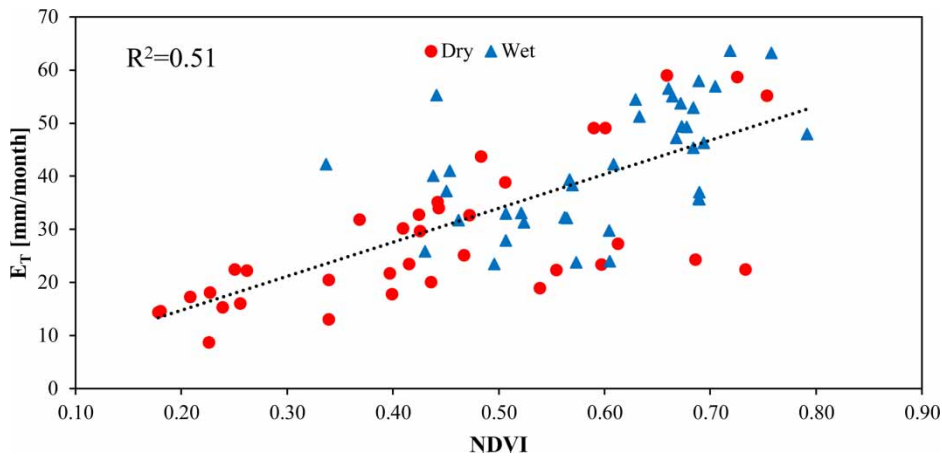


**Figure 12** | Scatter plot of monthly GG-NDVI  $E_T$  and NDVI from all 75 sites. The dashed line indicates a linear fit to the data.

**Table 5** | Comparison of performance using  $E_{RMS}$  (mm/month) between GG-NDVI and recently published results

Study	# of sites	Method	$E_{RMS}$ [mm/month]			$R^2$		
			Min	Max	Mean	Min	Max	Mean
This study	75	GG-NDVI	0.3	56.6	12.3	0.01	0.94	0.60
This study	75	Modified GG <sup>a</sup>	0.3	42.7	16.4	0.01	0.94	0.64
Mu <i>et al.</i> (2011)	46	MODIS <sup>b</sup>	9.4	52.0	25.6	0.02	0.93	0.65
Anayah & Kaluarachchi (2014)	34	Modified GG	10.3	59.9	20.6	0.01	0.94	0.64
Anayah & Kaluarachchi (2014)	34	CRAE	7.4	50.0	18.3	0.02	0.94	0.67
Han <i>et al.</i> (2011)	4	GG	3.7	16.0	10.7	0.82	0.98	0.92
Han <i>et al.</i> (2012)	4	GG	11.8	18.3	14.8			
Li <i>et al.</i> (2013)	26	Budyko	1.8	18.8	–			

<sup>a</sup>Anayah & Kaluarachchi (2014).<sup>b</sup>Remote sensing method.

studies. The mean  $E_{RMS}$  of GG-NDVI across the 75 sites produced the lowest  $E_{RMS}$  of 12.3 mm/month compared to 25.6 mm/month from a remote sensing method and 20.6 mm/month from the modified GG. It should be noted that both studies by Han *et al.* (2011, 2012) have only four sites. Although these studies evaluated other methods and were applied at different study sites, Mu *et al.* (2011) used the same data from AmeriFlux similar to this study and Li *et al.* (2013) used the Fu equation across 26 global river basins. A comparison of GG, the Fu equation, CRAE, and remote sensing methods with the GG-NDVI model shows that the proposed GG-NDVI is an enhancement to the modified GG model, providing improved predictions of  $E_T$  especially under dry conditions.

We plotted the GG-NDVI estimates of  $E_T$  against observed  $E_T$  and the same with the modified GG estimates for dry sites. The results are shown in Figure 13. In a linear regression analysis, the GG-NDVI model has greater strong agreement ( $R^2 = 0.60$ ) with observed  $E_T$  than modified GG model ( $R^2 = 0.46$ ). The GG-NDVI is, therefore, shown to be a reasonably good predictor of  $E_T$  and the  $R^2$  of 60% is much better than the recently published study of Allam *et al.* (2016) which is about 37%. In essence, the results show that GG-NDVI can improve performance under dry conditions.

## SUMMARY AND CONCLUSIONS

Models using the complementary method to estimate  $E_T$  are simple, practical, and provide valuable estimates of regional

$E_T$  using point meteorological data only. The methods do not require data such as soil moisture, stomatal resistance properties of vegetation, or any other aridity measures. Since the original work of Bouchet (1963), the complementary relationship has been the subject of many studies. Among the recent methods, Anayah & Kaluarachchi (2014) developed the modified GG model that is an enhanced version of the original GG method. It can be universally applied under a variety of climatic conditions without local calibration. While that study showed excellent results compared to the recently published work, the accuracy could be improved under dry conditions.

The Budyko framework has been successfully used to predict the long-term annual water balance as a function of  $E_p$  and precipitation. According to Yang *et al.* (2006), the Budyko hypothesis through the Fu equation is consistent with the Bouchet hypothesis which is based on the complementary relationship. Also, the Fu equation works well in dry conditions and it can be improved by using the vegetation cover represented by NDVI.

Given the limitation of not accurately predicting  $E_T$  under dry conditions, the goal of this work is to extend the modified GG model (Anayah & Kaluarachchi 2014) to combine the complementary relationship and the Budyko approach for improved estimation of  $E_T$ . The expectation is that this enhanced version of the GG model will produce better performance especially under dry conditions.

For the purpose of model development and application, 75 sites from the AmeriFlux database covering the United

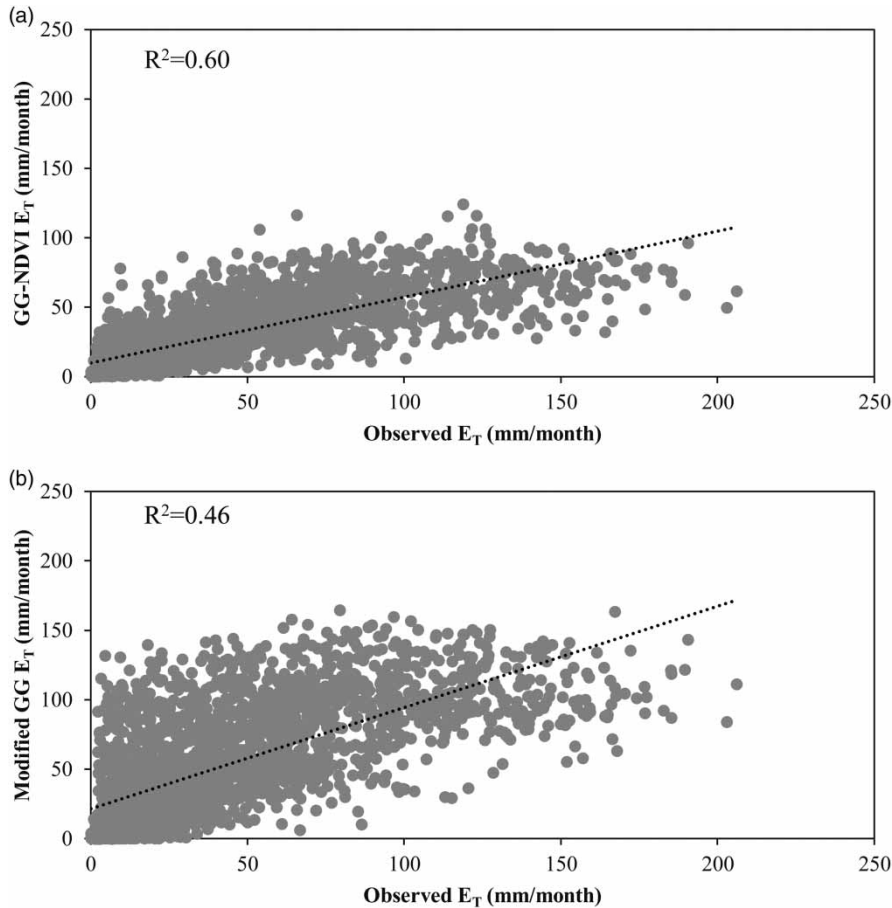


**Figure 13** | Scatter plot of monthly observed  $E_T$  and estimated  $E_T$  across 36 dry sites: (a) GG-NDVI and (b) modified GG. The dashed line indicates a linear fit to the data.

States were selected. These sites were divided based on an aridity index from UNEP (Barrow 1992), where 39 sites fall into the dry class and the remaining 36 the wet class. The GG-NDVI model shows better performance with both dry and wet sites compared to other methods. In general, the GG-NDVI model reduces mean  $E_{RMS}$  by about 24% compared to the modified GG model while increasing wetness leads to increasing accuracy with the GG-NDVI model. Lastly,  $E_T$  is directly proportional to the aridity index of dry sites. On the other hand, increasing of aridity index leads to decreasing  $E_T$  in wet sites. These trends were seen in recent studies from Roderick *et al.* (2009) and Han *et al.* (2014). The GG-NDVI model is more correlated with observed  $E_T$  than the modified GG model at values better than the work of Allam *et al.* (2016). Although this study applied the Budyko framework to the modified GG model, the GG-NDVI model shows similar results with other

complementary relationship studies as well. We may therefore conclude that the GG-NDVI model maintains the characteristics of both the complementary relationship and Budyko hypothesis. We also observed that  $E_T$  estimates of GG-NDVI have a good correlation coefficient with NDVI confirming conclusions from several previous studies (Hsiao & Henderson 1985; Bethenod *et al.* 2000; Hsiao & Xu 2005). However, when the vegetation cover is very dense or has a seasonal fluctuation, the proposed GG-NDVI model did not perform well. As a result, NDVI seems insufficient to represent plant transpiration, which suggests that other vegetation indices might be more suitable.

It is also noted that the GG-NDVI model requires NDVI and more computation than the modified GG model proposed by Anayah & Kaluarachchi (2014). However, NDVI data are readily available from satellite data from MODIS

or similar outlets. On a positive note, both GG-NDVI and modified GG require no local calibration. Reference  $E_T$  of FAO (Allen *et al.* 2005) is considered to be the best method and is widely used globally. Unfortunately, this method requires crop coefficients that vary depending on the growing season and crop type for different regions or countries. Lastly, this study will be the first to incorporate the vegetation cover to the complementary relationship through the Budyko framework to improve  $E_T$  predictions, especially under dry conditions. Consequently, the GG-NDVI model can be used as a powerful tool to estimate  $E_T$  with meteorological and remote sensing data at monthly time scale without local calibration.

## REFERENCES

- Allam, M. M., Jain-Figueroa, A., McLaughlin, D. B. & Eltahir, E. A. B. 2016 Estimation of evaporation over the Upper Blue Nile basin by combining observations from satellites and river flow gauges. *Water Resources Research* **52**, DOI:10.1002/2015WR017251.
- Allen, R. G., Pereira, L. S., Raes, D. & Smith, M. 1998 *Crop Evapotranspiration: Guidelines for Computing Crop Water Requirements*. FAO Irrigation and Drainage Paper No. 56. Food and Agriculture Organization of the United Nations, Rome, Italy.
- Allen, R. G., Walter, I. A., Elliot, R., Howell, T., Itenfisu, D. & Jensen, M. 2005 *The ASCE Standardized Reference Evapotranspiration Equation*. American Society of Civil Engineers Environmental and Water Resource Institute (ASCE-EWRI), American Society of Civil Engineers, Reston, VA, USA.
- Anayah, F. M. & Kaluarachchi, J. J. 2014 Improving the complementary methods to estimate evapotranspiration under diverse climatic and physical conditions. *Hydrology and Earth System Sciences* **18**, 2049–2064. DOI: 10.5194/hess-18-2049-2014.
- Barrow, C. J. 1992 *World Atlas of Desertification (United Nations Environment Programme) Section one: Global* (N. Middleton & D. S. G. Thomas, eds). Edward Arnold, London, UK.
- Bethenod, O., Katerji, N., Goujet, R., Bertolini, J. M. & Rana, G. 2000 Determination and validation of corn crop transpiration by sap flow measurement under field conditions. *Theoretical and Applied Climatology* **67**, 153–160.
- Bouchet, R. J. 1963 Evapotranspiration réelle et potentielle, signification climatique (Actual and potential evapotranspiration climate service). *International Association of Hydrological Sciences* **62**, 134–142.
- Brutsaert, W. & Stricker, H. 1979 An advection-aridity approach to estimate actual regional evapotranspiration. *Water Resources Research* **15** (2), 443–450.
- Budyko, M. I. 1974 *Climate and Life. Xvii*. Academic Press, New York, USA.
- Choudhury, B. J. 1999 Evaluation of an empirical equation for annual evaporation using field observations and results from a biophysical model. *Journal of Hydrology* **216**, 99–110.
- Crago, R. & Crowley, R. 2005 Complementary relationship for near-instantaneous evaporation. *Journal of Hydrology* **300**, 199–211.
- Fu, B. P. 1981 On the calculation of the evaporation from land surface. *Sci. Atmos. Sin.* **5** (1), 23–31 (in Chinese).
- Gerrits, A. M. J., Savenije, H. H. G., Veling, E. J. M. & Pfister, L. 2009 Analytical derivation of the Budyko curve based on rainfall characteristics and a simple evaporation model. *Water Resources Research* **45**, W04403. DOI:10.1029/2008WR007308.
- Granger, R. J. 1989 A complementary relationship approach for evaporation from nonsaturated surfaces. *Journal of Hydrology* **111**, 31–38. DOI:10.1016/0022-1694(89)90250-3.
- Granger, R. J. & Gray, D. M. 1989 Evaporation from natural non-saturated surface. *Journal of Hydrology* **111**, 21–29. DOI:10.1016/0022-1694(89)90249-7.
- Han, S., Hu, H. & Yang, D. 2011 A complementary relationship evaporation model referring to the Granger model and the advection-aridity model. *Hydrological Processes* **25** (13), 2094–2101.
- Han, S., Hu, H. & Tian, F. 2012 A nonlinear function approach for the normalized complementary relationship evaporation model. *Hydrological Processes* **26** (26), 3973–3981.
- Han, S., Tian, F. & Hu, H. 2014 Positive or negative correlation between actual and potential evaporation? Evaluating using a nonlinear complementary relationship model. *Water Resources Research* **50**, 1322–1336. DOI:10.1002/2013WR014151.
- Hobbins, M. T., Ramirez, J. A., Brown, T. C. & Classens, L. H. J. M. 2001 The complementary relationship in estimation of regional evapotranspiration: the complementary relationship areal evapotranspiration and advection-aridity models. *Water Resources Research* **37** (5), 1367–1387.
- Hsiao, T. C. & Henderson, D. W. 1985 *Improvement of Crop Coefficients for Evapotranspiration, Final Report. California Irrigation Management Information System project*, Vol. 1, Land, Air & Water Resources Papers 10013-A, University of California Davis, CA, USA, pp. III3–III35.
- Hsiao, T. C. & Xu, L. 2005 *Evapotranspiration and Relative Contribution by the Soil and the Plant. California Water Plan Update 2005*, University of California Davis, CA, USA.
- Huete, A. R. 1988 A soil-adjusted vegetation index (SAVI). *Remote Sensing of Environment* **25**, 295–309.
- Kahler, D. M. & Brutsaert, W. 2006 Complementary relationship between daily evaporation in the environment and pan evaporation. *Water Resources Research* **42**, W05413. DOI:10.1029/2005WR004541.
- Li, D., Pan, M., Cong, Z., Zhang, L. & Wood, E. 2013 Vegetation control on water and energy balance within the Budyko framework. *Water Resources Research* **49**, 969–976. DOI:10.1002/wrcr.20107.

- Monteith, J. L. 1965 Evaporation and environment. In: *19th Symp. Soc. Exp. Biol.* University Press, Cambridge, pp. 205–234.
- Morton, F. I. 1985 Operational estimates of areal evapotranspiration and their significance to the science and practice of hydrology. *Journal of Hydrology* **66**, 1–76.
- Morton, F. I. 1994 Evaporation research – a critical review and its lessons for the environmental sciences. *Critical Reviews in Environmental Science and Technology* **24** (3), 237–280.
- Mu, Q., Zhao, M. & Running, S. W. 2007 Development of a global evapotranspiration algorithm based on MODIS and global meteorological data. *Remote Sensing of Environment* **111** (4), 519–536. DOI:10.1016/J.RSE.2007.04.015.
- Mu, Q., Zhao, M. & Running, S. W. 2011 Improvements to a MODIS global terrestrial evapotranspiration algorithm. *Remote Sensing of Environment* **115**, 1781–1800. DOI:10.1016/J.RSE.2011.02.019.
- Penman, H. L. 1948 Natural evaporation from open water, bare and grass. *Proceedings of the Royal Society A: Mathematical, Physical and Engineering Sciences* **193** (1032), 120–145. DOI:10.1098/rspa.1948.0037.
- Pettorelli, N., Vik, J. O., Mysterud, A., Gaillard, J. M., Tucker, C. J. & Stenseth, N. C. 2005 Using the satellite-derived NDVI to assess ecological responses to environmental change. *Trends in Ecology and Evolution* **20** (9), 503–510. DOI:10.1016/j.tree.2005.05.011.
- Pike, J. G. 1964 The estimation of annual runoff from meteorological data in a tropical climate. *Journal of Hydrology* **2**, 116–123.
- Potter, N. J., Zhang, L., Milly, P. C. D., McMahon, T. A. & Jakeman, A. J. 2005 Effects of rainfall seasonality and soil moisture capacity on mean annual water balance for Australian catchments. *Water Resources Research* **41**, W06007. DOI:10.1029/2004WR003697.
- Priestley, C. H. B. & Taylor, R. J. 1972 On the assessment of surface heat fluxes and evaporation using large-scale parameters. *Monthly Weather Review* **100**, 81–92.
- Roderick, M. L., Hobbins, M. T. & Farquhar, G. D. 2009 Pan evaporation trends and the terrestrial water balance. II: Energy balance and interpretation. *Geography Compass* **3** (2), 761–780.
- Shuttleworth, W. J. 2006 Towards one-step estimation of crop water requirements. *Transactions of the ASABE* **49** (4), 925–935.
- Shuttleworth, W. J. & Wallace, J. S. 2009 Calculating the water requirements of irrigated crops in Australia using the Matt-Shuttleworth approach. *Transactions of the ASABE* **52** (6), 1895–1906.
- Suleiman, A. & Crago, R. 2004 Hourly and daytime ET from grassland using radiometric surface temperatures. *Agronomy Journal* **96**, 384–390.
- Szilagyi, J. & Jozsa, J. 2008 New findings about the complementary relationship based evaporation estimation methods. *Journal of Hydrology* **354**, 171–186.
- Szilagyi, J. & Kovacs, A. 2010 Complementary-relationship-based evapotranspiration mapping (cremap) technique for Hungary. *Periodica Polytechnica: Civil Engineering* **54** (2), 95–100. DOI:10.3311/pp.ci.2010.2.04.
- Thompson, S. E., Harman, C. J., Konings, A. G., Sivapalan, M., Neal, A. & Troch, P. A. 2011 Comparative hydrology across AmeriFlux sites: the variable roles of climate, vegetation, and groundwater. *Water Resources Research* **47**, W00J07. DOI:10.1029/2010WR009797.
- Venturini, V., Islam, S. & Rodríguez, L. 2008 Estimation of evaporative fraction and evapotranspiration from MODIS products using a complementary based model. *Remote Sensing of Environment* **112**, 132–141.
- Venturini, V., Rodríguez, L. & Bisht, G. 2011 A comparison among different modified Priestley and Taylor's equation to calculate actual evapotranspiration. *International Journal of Remote Sensing* **32** (5), 1319–1338. DOI:10.1080/01431160903547965.
- Xu, C. Y. & Singh, V. P. 2005 Evaluation of three complementary relationship evapotranspiration models by water balance approach to estimate actual regional evapotranspiration in different climate regions. *Journal of Hydrology* **308**, 105–121.
- Yang, D., Sun, F., Liu, Z., Cong, Z. & Lei, Z. 2006 Interpreting the complementary relationship in non-humid environments based on the Budyko and Penman hypotheses. *Geophysical Research Letters* **33**, L18402. DOI:10.1029/2006GL027657.
- Yang, D., Sun, F., Liu, Z., Cong, Z., Ni, G. & Lei, Z. 2007 Analyzing spatial and temporal variability of annual water energy balance in non humid regions of China using the Budyko hypothesis. *Water Resources Research* **43**, W04426. DOI:10.1029/2006WR005224.
- Yang, H. B., Yang, D. W., Lei, Z. D. & Sun, F. B. 2008 New analytical derivation of the mean annual water-energy balance equation. *Water Resources Research* **44** (3), W03410. DOI:10.1029/2007WR006135.
- Yang, D., Shao, W., Yeh, P. J. F., Yang, H., Kanae, S. & Oki, T. 2009 Impact of vegetation coverage on regional water balance in the nonhumid regions of China. *Water Resources Research* **45**, W00A14. DOI:10.1029/2008WR006948.
- Yuan, W. P., Liu, S. G., Yu, G. R., Bonnefond, J. M., Chen, J. Q., Davis, K., Desai, A. R., Goldstein, A. H., Gianelle, D., Rossi, F., Suyker, A. E. & Verma, S. B. 2010 Global estimates of evapotranspiration and gross primary production based on MODIS and global meteorology data. *Remote Sensing of Environment* **114** (7), 1416–1431.
- Zhang, L., Dawes, W. R. & Walker, G. R. 2001 Response of mean annual evapotranspiration to vegetation changes at catchment scale. *Water Resources Research* **37** (3), 701–708.
- Zhang, L., Hickel, K., Dawes, W. R., Chiew, F. H. S., Western, A. W. & Briggs, P. R. 2004 A rational function approach for estimating mean annual evapotranspiration. *Water Resources Research* **40**, 02502. DOI:10.1029/2003WR002710.

First received 17 October 2016; accepted in revised form 3 May 2017. Available online 16 June 2017